

Caspase Cascade Regulated Mitochondria Mediated Apoptosis in Monocrotophos Exposed PC12 Cells

M. P. Kashyap,[†] A. K. Singh,[†] M. A. Siddiqui,^{†,§} V. Kumar,[†] V. K. Tripathi,[†]
V. K. Khanna,[†] S. Yadav,[†] S. K. Jain,[‡] and A. B. Pant^{*,†}

Indian Institute of Toxicology Research, Lucknow, India, Council of Scientific & Industrial Research, New Delhi, India, and Department of Biotechnology, Jamia Hamdard University, New Delhi, India

Received December 17, 2009

Monocrotophos (MCP) is a commonly used organophosphorus (OP) pesticide. We studied apoptotic changes in PC12 cells exposed to MCP. A significant induction in reactive oxygen species (ROS), lipid peroxide (LPO), and the ratio of glutathione disulfide (GSSG)/reduced glutathione (GSH) was observed in cells exposed to selected doses of MCP. Following the exposure of PC12 cells to MCP, the levels of protein and mRNA expressions of Caspase-3, Caspase-9, Bax, p53, P²¹, Puma, and cytochrome-*c* were significantly upregulated, whereas the levels of Bcl₂, Bcl_w, and Mcl1 were downregulated. TUNEL assay, DNA laddering, and micronuclei induction show that long-term exposure of PC12 cells to MCP at higher concentration (10⁻⁵ M) decreases the number of apoptotic events due to an increase in the number of necrotic cells. MCP-induced translocation of Bax and cytochrome-*c* proteins between the cytoplasm and mitochondria confirmed the role of p53 and Puma in mitochondrial membrane permeability. Mitochondria mediated apoptosis induction was confirmed by the increased activity of caspase cascade. We believe that this is the first report showing MCP-induced apoptosis in PC12 cells, which is mitochondria mediated and regulated through the caspase cascade. Our data demonstrates that MCP induced the apoptotic cell death in neuronal cells and identifies the possible cellular and molecular mechanisms of organophosphate pesticide-induced apoptosis in neuronal cells.

Introduction

Toxicological consequences of pesticides are well documented in both environmental and occupational setups (1, 2). The organophosphorus (OP) group of pesticides have been used extensively across the globe for more than five decades (3) resulting in an annual exposure to 2–3 million people (4). Both acute and chronic exposures of OPs are known to induce toxicity in mammalian systems (5–8). OPs primarily act by inhibiting acetyl cholinesterase (AChE) activity in the neuronal system (9–11). However, the toxicological responses of OP compounds have also been linked with necrosis (12, 13), apoptosis (14), and oxidative stress-mediated pathways (14, 15). OP-induced oxidative stress in the developing brain has also been reported to alter the expression and functions of antioxidant genes (16, 17). It is apparent from these reports that the behavioral deficits or toxic responses for various OPs may be different, in part, due to the involvement of different mechanisms that contribute to the net adverse outcomes (17, 18).

In order to understand the mechanisms of OPs-induced toxicity, studies have been carried out in cultured cells using end points such as DNA fragmentation (2), neutral red uptake (19), protein synthesis inhibition (9), released lactate dehydrogenase, trypan blue dye exclusion, ADP/ATP ratio (13), impaired cell growth, glucose metabolism (20), and morphologi-

cal changes (21). The knowledge of specific mechanisms involved in specific OP-induced toxicity is limited; however, the involvement of apoptotic cascade has been suggested (2). Apoptotic cell death is regulated by different signaling pathways under in vitro (22, 23) and in vivo (24, 25) conditions. Moreover, different OPs have shown apoptosis induction via different pathways (2, 14, 17).

It is therefore important to study the exact mechanism(s) involved in the toxicity of these pesticides. Thus, the present investigation was designed to study the pathway(s) involved in monocrotophos (MCP¹)-induced apoptotic cell death in cultured PC12 cells, a rat pheochromocytoma cell line. MCP was selected as a model pesticide in the study since it has been used extensively in many parts of the world including India for more than forty years and is known for its systemic toxicity including neurotoxicity (26–28). PC12 cells were selected because most marker genes associated with neurotoxicity (29), apoptosis (30), necrosis (31), and cell cycles (32) are easily expressed and induced in these cells.

¹ Abbreviations: PC12 cell line, rat pheochromocytoma cell line; NF-12 medium, nutrient mixture (F-12 Hams); FBS, fetal bovine serum; HS, horse serum; NaHCO₃, sodium bicarbonate; MCP, dimethyl (*E*)-1-methyl-2-methyl carbanoyl vinyl phosphate (C7H14NO5-P); bisbenzimidazole, (2'-[4-ethoxyphenyl]-5-[4-methyl-1-piperazinyl]-2,5'-bi-1*H*-benzimidazole); NRU, Neutral Red uptake; LDH, lactate dehydrogenase; DCFH-DA, 2',7'-dichlorodihydrofluorescein-diacetate; DCF, dichlorofluorescein; PLL, poly L-lysine; PBS, phosphate buffered saline; GSH, glutathione (reduced form); GSH-Px, glutathione peroxidase; GSSG, glutathione (oxidized form); Gsr, glutathione reductase; LPO, lipid peroxidation; MTT, 3-(4,5-dimethylthiazol-2-yl)-2,5-diphenyltetrazoliumbromide; ROS, reactive oxygen species; MN assay, micronucleus assay; TUNEL, deoxynucleotide transferase dUTP nick end labeling; BCA, bicinonchonic acid; PVDF, polyvinylidene fluoride; TMB, 3,3',5,5'-tetramethyl bezidine; TP53, tumor protein 53; Bcl₂, B cell lymphoma 2; TdT, terminal deoxynucleotidyl transferase; BrdUTP, 5-bromo-2'-deoxyuridine 5'-triphosphate; EMS, ethyl methyl sulfonate.

* Corresponding author. *In Vitro* Toxicology Laboratory, Indian Institute of Toxicological Research, P. O. Box 80, MG Marg, Lucknow-226001, India. Phone: +91-522-2627586 (work); +91-9935044044 (personal). Fax: +91-522-2628227. E-mail: abpant@rediffmail.com; abpant@yahoo.com.

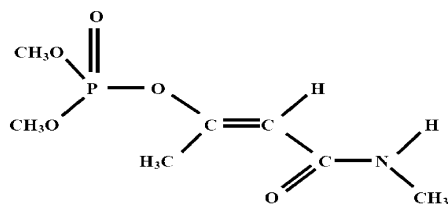
[†] Indian Institute of Toxicology Research.

[‡] Jamia Hamdard University.

[§] Present address: DNA Research Chair, Department of Zoology, College of Science, King Saud University, Riyadh, Saudi Arabia.

Materials and Methods

Chemical Structure of Monocrotophos.



Dimethyl (E)-1-methyl-2-methyl carbanoyl vinyl phosphate (C7H14NO5-P)

Cell Culture. PC12 cells were originally procured from National Centre for Cell Sciences, Pune, India, and have been maintained at In Vitro Toxicology Laboratory, Indian Institute of Toxicology Research, Lucknow, India, as per the standard protocols. Briefly, cells were cultivated in Nutrient Mixture (F-12 Hams), supplemented with 2.5% fetal bovine serum (FBS), 15% horse serum (HS), 0.2% sodium bicarbonate (NaHCO_3), 100 units/mL penicillin G sodium, 100 $\mu\text{g}/\text{mL}$ streptomycin sulfate, and 0.25 $\mu\text{g}/\text{mL}$ amphotericin B. Cultures were maintained at 37 °C in 5% CO_2 –95% atmosphere under high humidity. The culture medium was changed twice weekly, and cultures were passaged at a ratio of 1:6 once a week. Prior to experiments, cells were checked for their viability using the trypan blue dye exclusion assay following the protocol of Pant et al., (33, 34), and batches showing more than 95% viability were used.

Reagents and Consumables. All of the specified chemicals, primers, probes, and reagents, viz., MCP (dimethyl (E)-1-methyl-2-methyl carbanoyl vinyl phosphate (IUPAC) C7H14NO5-P; catalog no. PS-609; purity 99.5%), and diagnostic kits were purchased from Sigma Chemical Company Pvt. Ltd. St. Louis, MO, USA, unless otherwise stated. Culture medium nutrient mixture F-12 Hams, antibiotics, and fetal bovine and horse sera were purchased from Gibco BRL, USA.

Lipid Peroxidation (LPO). Following the exposure of MCP (10^{-4} – 10^{-6} M) for 6, 12, and 24 h, cells were harvested by centrifugation at 1000 rpm for 10 min and processed for the estimation of lipid peroxidation using a commercially available kit (Lipid Peroxidation Assay Kit, catalog no. 705003; Cayman Chemicals, USA) as per the manufacturer's protocol. Cells exposed to H_2O_2 (100 μM) for 2 h under identical conditions served as the positive control.

Ratio of Glutathione Disulfide/Reduced Glutathione. The ratio of glutathione disulfide (GSSG) with respect to reduced glutathione (GSH) was assessed under the same experimental setup as that of LPO using a commercially available kit (ApoGSH Glutathione Colorimetric Assay Kit, catalog no. K261-100, Biovision, USA). The data are presented by calculating the ratio between GSSG and GSH. Cells exposed to H_2O_2 (100 μM) for 2 h under identical conditions were used as the positive control.

Reactive Oxygen Species (ROS) Generation. MCP-induced ROS generation in PC12 cells was assessed using 2',7'-dichlorodihydrofluorescein diacetate (DCFH-DA; Sigma Aldrich, USA) dye as the fluorescence agent (35). Briefly, cells (5×10^4 per well) were seeded in poly L-lysine precoated tissue culture slide flasks and allowed to adhere. Adhered cells were then exposed to various concentrations of MCP (10^{-5} M to 10^{-7} M) for 6 h. Following exposure, cells were washed twice with PBS and incubated for 30 min in the dark in incomplete culture medium containing DCFH-DA (20 μM). Slides were washed twice with PBS and mounted for microscopic analysis. Intracellular fluorescence was measured using an upright fluorescence microscope by grabbing the images (Nikon Eclipse 80i equipped with Nikon DS-Ri1 12.7 megapixel camera). Quantification of fluorescence was done using the image analysis software Leica Qwin 500, and data were expressed as the fold change of unexposed control. Cells exposed to H_2O_2 (100 μM) for 2 h under identical conditions were used as a positive control.

TUNEL Assay. Apoptosis during the cell cycle was detected by deoxynucleotide transferase dUTP nick end labeling (TUNEL),

and propidium iodide (PI)/RNase staining assays using APO-BrdU TUNEL Assay Kit with Alexa Fluor 488 anti-BrdU (Molecular Probes, Invitrogen detection Technologies, USA, catalog no. A23210) by a flow cytometer (BD-FACS Canto, USA) equipped with BD FACS Diva, version 6.1.2, software. Debris was excluded by forward and side-way light-scattering. The role of ROS in the induction of apoptosis was ascertained by using the ROS inhibitor, diphenyleneiodonium chloride (DPI) (10 μM), 1 h prior to the exposure of MCP (10^{-5} M) for 6 h. Positive and negative controls were provided with the kit. Cells exposed to camptothecin (3 $\mu\text{g}/\text{mL}$) for 6 h were also used as positive controls.

DNA Laddering. MCP-induced apoptotic alterations were also observed by DNA fragmentations using an enhanced apoptotic DNA ladder detection kit (catalog no. K130-50, Biovision, USA). DNA fragmentations were studied for apoptosis and necrosis under UV illumination in Gel Documentation System (Alpha Innotech, USA).

Micronucleus Induction (MN Assay). Micronucleus (MN) assay was carried out using standard protocol (36) with some modifications tailored for PC12 cells. Briefly, following the exposure of MCP (10^{-4} – 10^{-6} M) for 6, 12, and 24 h, cells were incubated up to 43–44 h in fresh medium and blocked for cytokinesis using cytochalasin-B (3 $\mu\text{g}/\text{mL}$, Sigma, USA). Cells were then harvested by hypotonic buffer (0.075 M KCl) for 5–10 min at 37 °C and fixed in Carnoy's fixative (methanol/acetic acid, 3:1). Finally, cells were dropped onto the slides and stained with 5% Giemsa in phosphate buffer (pH 6.8) for 15–20 min and mounted with DPX for microscopic examination. A minimum of 1000 binucleated cells with well-defined cytoplasm in each slide were scored for the presence of MN using a Nikon Eclipse 80i upright microscope attached with a Nikon digital CCD cool camera (Model DS-Ri1 of 12.7 Megapixel). Data presented for MN are the mean of three slides. Ethyl methyl sulfonate (2 mM) was used as the positive control.

Transcriptional Changes. Transcriptional changes in marker genes associated with oxidative stress and apoptosis mediated pathways were studied following MCP (10^{-6} M) exposure for 6 h. Total RNA was isolated from both experimental and unexposed control sets using GeneElute mammalian total RNA Miniprep Kit (catalog no. RTN-70, Sigma, USA). Total RNA (1 μg) was reverse-transcribed into cDNA by SuperScript III first strand cDNA synthesis kit (catalog no. 18080-051, Invitrogen Life Science, USA). Quantitative real time PCR (RT-PCR^q) was performed by SYBR Green dye (ABI, USA) using ABI PRISM 7900HT Sequence Detection System (Applied Biosystems, USA). Real time reactions were carried out in triplicate wells for each sample. Sequences of different primers are given in Table S-1 (Supporting Information). The specificity of each primer was assessed by melting curve analysis and NTCs for respective primers. Actin- β was used as an internal control to normalize the data. MCP-induced alterations are expressed in relative quantification.

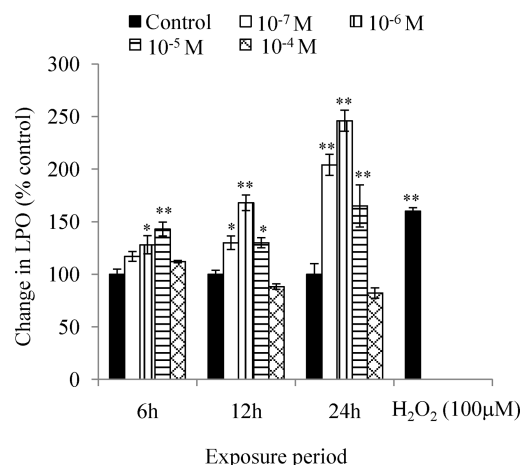


Figure 1. Lipid peroxidation (LPO) in PC12 cells following the exposure of MCP for various time periods. Exposure of 100 μM H_2O_2 for 2 h was used as the positive control. * = $P < 0.05$; ** = $p < 0.001$.

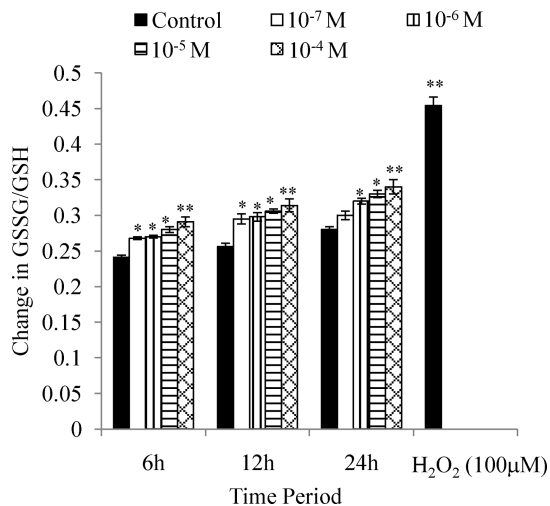


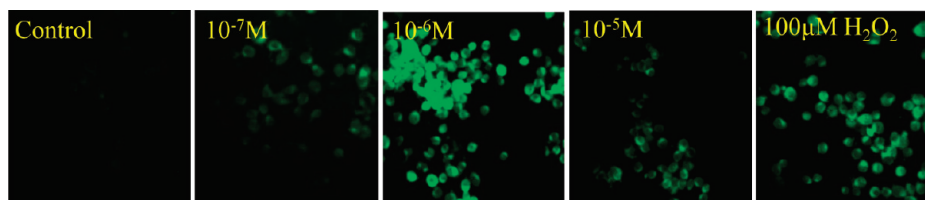
Figure 2. Ratio of glutathione disulfide (oxidized form of glutathione) with respect to reduced glutathione (GSSG/GSH) in PC12 cells following the exposure of MCP for various time periods. Exposure of 100 μM H₂O₂ for 2 h was used as the positive control. * = *P* < 0.05; ** = *P* < 0.001.

Translational Changes. PC12 cells were exposed to MCP (10⁻⁶ M) for 6, 12, and 24 h. Western blot analysis was carried out for selected apoptosis marker proteins (p53, Bax, Bcl₂, activated Caspase 3 and 9, and early response genes viz. C-fos and C-jun). Briefly, following MCP exposure, cells were pelleted and lysed using CellLytic M Cell Lysis Reagent (catalog no. C2978, Sigma, USA) in the presence of 1× protein inhibitor cocktail (catalog no. P8340, Sigma, USA). Protein estimation was done by BCA Protein Assay Kit (catalog no. G1002, Lamda Biotech, Inc., St. Louis, MO, USA). Equal amounts (50 μg/well) of proteins were loaded in 10% tricine-SDS gel (37) and blotted on polyvinylidene fluoride (PVDF) membranes using wet transfer system. After blocking for 2 h at 37 °C, the membranes were incubated overnight at 4 °C with antiprotein primary antibodies specific for p53 (1:1000, BD Biosciences, USA), Bax, C-jun, and C-fos (1:500, Santa Cruz,

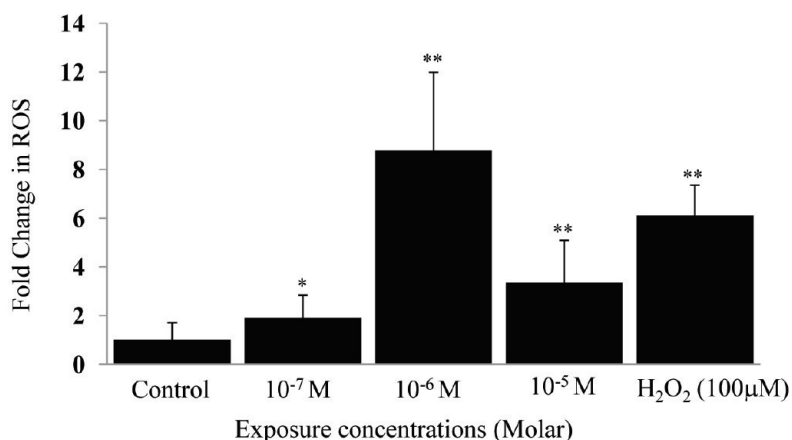
USA), Bcl₂, activated Caspase 3 and 9 (1:1000, CST, USA), and Actin-β (1:2000, Santa Cruz, USA) in blocking buffer (pH 7.5). The membrane was then incubated for 2 h at room temperature with secondary antiprimary immunoglobulin G (IgG)-conjugated with horseradish peroxidase (Calbiochem, USA). The blots were developed using either luminol (catalog no. 34080, Thermo Scientific, USA) or by TMB-H₂O₂ (Sigma, USA), and densitometry for protein specific bands was done in Gel Documentation System (Alpha Innotech, USA) with the help of AlphaEase FC StandAlone V. 4.0.0 software. Actin-β was used as an internal control to normalize the data. MCP-induced alterations are expressed in relative quantities (fold change) by comparing the data with respective unexposed controls. Self-recovery in the altered expressions were also studied by incubating MCP-exposed (6 h) cells for another 18 h in culture medium without MCP supplementation.

Translocation Studies. Translocation of Bax protein from cytosol to mitochondria and cytochrome-*c* from mitochondria to cytosol due to MCP-induced mitochondrial membrane permeabilization (MMP) was studied by Western blot analysis using specific anti-Bax and anticytochrome-*c* primary antibodies (Santa Cruz, USA). Following the exposure of MCP (10⁻⁴–10⁻⁷ M) for 6 h, cells were harvested and processed for isolation of mitochondrial and cytosolic fractions using the protocols of Ghosh et al. (38) and Waterhouse et al. (39), respectively. The cross-contamination of cytosolic protein in the mitochondrial fraction and vice versa was also assessed by running separate blots using antibodies specific to mitochondria and cytosolic proteins.

Caspase-9 and Caspase-3. MCP-induced alterations in the activity of caspase-9 and caspase-3 were monitored using kits (Calbiochem, catalog no. QIA72, USA and Biovision, catalog no. K196, USA, respectively). Following MCP exposure, cells were pelleted, resuspended in prechilled extraction buffer (50 μL), and incubated for 10 min on ice. Then, the samples were centrifuged for 5 min at 500g and the clear supernatant (50 μL per well) transferred to black bottomed 96-well culture plates for Caspase-9, and clear plates for Caspase-3. Assay buffer (50 μL) and substrate conjugate (10 μL) for Caspase-9 and (5 μL) for Caspase-3 was added and mixed well. Immediately after the completion of 2 h of incubation at 37 °C in dark, contents were mixed thoroughly and



(a)



(b)

Figure 3. (a) Representative microphotographs showing MCP induced reactive oxygen species (ROS) generation in PC12 cells. ROS generation was studied using dichlorofluorescein diacetate (DCFH-DA) dye. Images were grabbed in Nikon phase contrast cum fluorescence microscope (model 80i), and quantification of fluorescence was done using Leica Q win500 image analysis software. Exposure of 100 μM H₂O₂ for 2 h was used as positive control. (b) Relative quantification of fold induction in ROS generation following 6 h of exposure of various concentrations of MCP in PC12 cells assessed by intracellular image analysis.

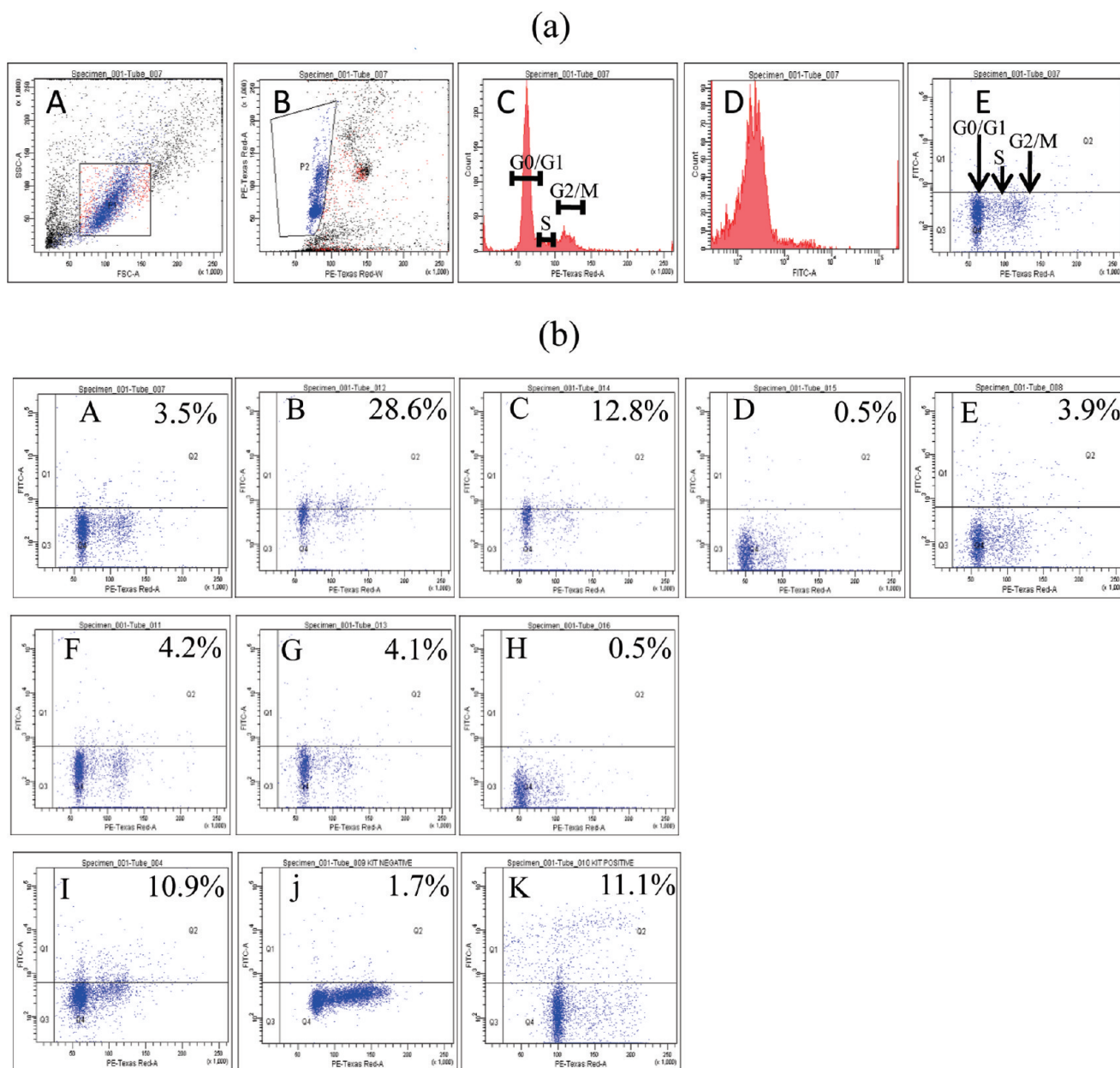


Figure 4. (a) Validation studies for TUNEL assay were carried out in PC12 cells by the APO-BrdU TUNEL assay kit using Cytometer (BD-FACS Canto, USA) equipped with BD FACS Diva, version 6.1.2 software. (A) Gating of the desired population of PC12 cells (P-1); (B) gating of single cells from the desired cell population, i.e., segregation of clumped cells; (C) cell cycle analysis in segregated desired population of PC12 cells; (D) analysis of apoptotic events by quantification of DNA nick in PC12 cells with the help of APO-BrdU TUNEL Assay Kit with Alexa Fluor 488 anti-BrdU (Molecular Probes, Invitrogen detection Technologies, USA; catalog no. A23210); and (E) analysis of cell cycle and apoptosis in PC12 cells. (b) MCP induced alterations in DNA fragmentation and cell cycle analysis in PC12 cells using APO-BrdU TUNEL Assay Kit with Alexa Fluor 488 anti-BrdU (Molecular Probes, Invitrogen detection Technologies, USA; catalog no. A23210). (A) Control cells; (B) MCP (10^{-5} M) treated cells for 6 h; (C) MCP (10^{-5} M) treated cells for 12 h; (D) MCP (10^{-5} M) treated cells for 24 h; (E) cells pretreated with ROS inhibitor, diphenyleneiodonium chloride (DPI), ($10 \mu\text{M}$) for 1 h followed by an exposure of MCP (10^{-5} M) for 6 h; (F) MCP (10^{-6} M) treated cells for 6 h; (G) MCP (10^{-6} M) treated cells for 12 h; (H) MCP (10^{-6} M) treated cells for 24 h; (I) cells treated with camptothecin ($3 \mu\text{g}/\text{mL}$) for 6 h as the experimental positive control; (J) negative control cells (human lymphoma cell line) provided with the kit; and (K) positive control cells (human lymphoma cells) provided with the kit. Values provided in each quadrant (Q2) depict the percent apoptosis during different phases of the cell cycle.

read for fluorescence at 400 nm excitation and 505 nm emission wavelength for Caspase-9, and for absorbance at 400 nm for Caspase-3. The values of exposed groups were compared with unexposed control sets and the data expressed as a percent of control.

Statistical Analysis. Results are expressed as the mean \pm SEM from the values obtained from at least three independent experiments, and triplicates samples were used in each experiment. Statistical analyses were performed using one-way analysis of variance (ANOVA) and post hoc Dunnett's (two sided) test to compare the findings in different groups. The values, $p < 0.05$, were considered significant.

Results

Lipid Peroxidation (LPO). Results of MCP-induced lipid peroxidation in PC12 cells are presented in Figure 1. A time-dependent significant induction in LPO was observed for MCP exposure of 10^{-7} M ($117 \pm 4.7\%$, $130 \pm 6.4\%$, and $204 \pm 10\%$) and 10^{-6} M ($128 \pm 8.7\%$, $168 \pm 7.4\%$, and $246 \pm 10\%$) at 6, 12, and 24 h, respectively. 10^{-5} M MCP exposure shows a biphasic response at 6 h ($143 \pm 6.7\%$), 12 h ($130 \pm 4.9\%$), and 24 h ($165 \pm 20\%$); however, the difference in values was not significant at 6 and 12 h. The lower values of LPO induction

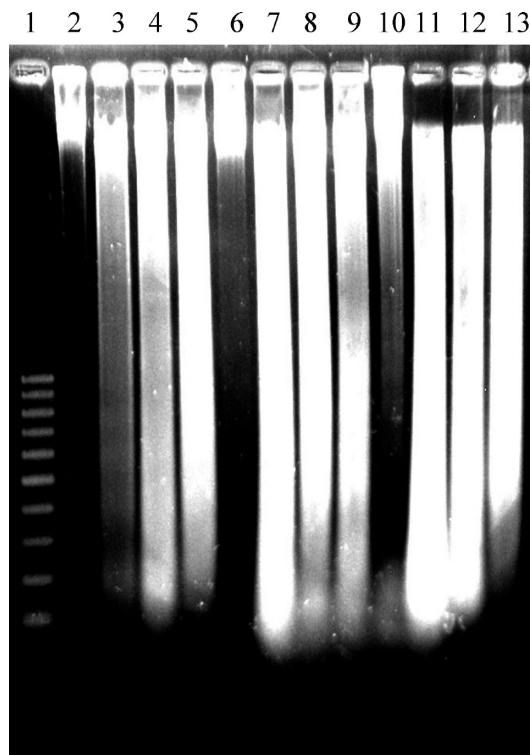


Figure 5. Analysis of apoptotic DNA fragmentation in PC12 cells exposed to various concentrations of MCP for different time intervals. Lane 1, 100 bp ladder; lane 2, untreated control cells; lanes 3, 4, and 5, cells exposed to MCP (10^{-6} M, 10^{-5} M, and 10^{-4} M, respectively) for 6 h; lane 6, untreated control; lanes 7, 8, and 9, cells exposed to MCP (10^{-6} M, 10^{-5} M, and 10^{-4} M, respectively) for 12 h; lane 10, untreated control; and lanes 11, 12, and 13, cells exposed to MCP (10^{-6} M, 10^{-5} M, and 10^{-4} M, respectively) for 24 h.

were observed for MCP (10^{-5} and 10^{-4} M), consistent with the diminished viability shown in Figure 1.

Ratio between Glutathione Disulfide (GSSG) and Glutathione Levels. MCP-induced alterations in the ratio between GSSG and GSH are summarized in Figure 2. A statistically significant increase in the ratio was observed in a dose- and time-dependent manner for all the concentrations of MCP used except for 10^{-7} M at 24 h.

ROS Generation. The statistically significant ($p < 0.001$) ROS generation was observed in PC12 cells receiving MCP (10^{-5} M– 10^{-7} M) for 6 h (Figure 3a–b). MCP (10^{-6} M) exposure induced a maximum of 8.77 ± 3.2 -fold increase in ROS followed by 3.35 ± 1.7 -fold (10^{-5} M) and 1.9 ± 0.92 -fold (10^{-7} M) MCP.

TUNEL Assay. MCP-induced apoptosis was assessed using the TUNEL assay with the help of FACS analysis (Figure 4a and b). The significant ($p < 0.001$) apoptotic changes, i.e., 28.6% were observed in early exposure of MCP (10^{-5} M) for 6 h. These changes were brought down to 12.8% after 12 h. Pretreatment of cells with ROS inhibitor restricted the apoptotic events close to the control, i.e., 3.9% following 6 h of exposure to MCP (10^{-5} M). Insignificant increases in apoptosis were observed in cells exposed to MCP (10^{-6} M) for 6 h (4.2%) and 12 h (4.1%). Apoptotic events were observed below the untreated control, i.e., 0.5% in cells exposed to MCP (10^{-5} M and 10^{-6} M) for 24 h. All of the subphases of cell cycles, i.e., G1, S, G2, and M were found to be involved in MCP-induced apoptosis in PC12 cells (Figure 4a and b).

DNA Laddering. DNA laddering of cells exposed to MCP (10^{-4} M– 10^{-6} M) for 6, 12, and 24 h are presented in Figure 5. A significant dose-dependent DNA smearing was observed

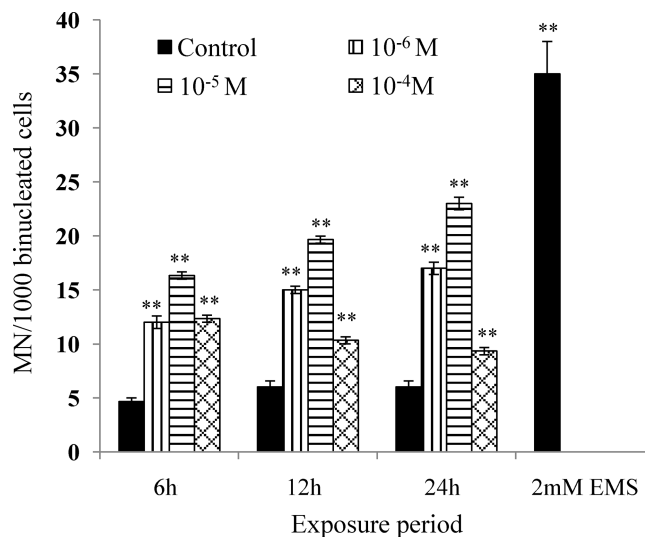


Figure 6. Micronuclei (MN) induction in PC12 cells exposed to various concentrations of MCP for different time periods. Micronuclei were counted in binucleated cells using an Upright phase contrast microscope (Nikon 80i, Japan) at $10 \times 100\times$ oil immersion magnification, and images were grabbed by a Nikon DS-Ri1 (12.7 megapixel) camera. Minimum 1000 binucleated cells were counted in each slide in triplicate. Ethyl methyl sulfonate (EMS) was used as the positive control. * $p < 0.05$; ** $p < 0.001$.

even at 6 h of MCP exposure (lanes 3, 4, and 5), which became more prominent by 12 h (7–9). However, the effect was concentration-independent at 12 h. MCP exposure for 24 h showed the signs of necrosis, as no high molecular weight DNA was seen in the upper side of lanes 11, 12, and 13. The trends were similar to those observed in the case of the TUNEL assay.

Micronucleus (MN) Assay. Results of MN induction in PC12 cells are shown in Figure 6. The influence of both MCP exposure time and concentration was observed on the induction of MN in PC12 cells except for 10^{-4} M. Among the concentrations of MCP used, 10^{-5} M was found to induce maximum MN at all of the time points, i.e., 6 h (16.3 ± 0.33), 12 h (19.66 ± 0.33), and 24 h (23.0 ± 0.58). Cells exposed to 10^{-6} M MCP have also shown time-dependent increases in MN, i.e., 12 ± 0.557 , 15.0 ± 0.33 , and 17.0 ± 0.33 at 6 h, 12 h, and 24 h, respectively. In contrast, the MN count was found to be reduced with increasing cell exposure time periods to 10^{-4} M MCP. However, the values were still greater than the unexposed control cells throughout the experimental period (Figure 6).

Transcriptional Changes. MCP-induced alterations in the mRNA expression of apoptosis marker genes are presented in Figure 7. Significant ($p < 0.001$) upregulation in the expression of pro-apoptotic genes, i.e., Caspase 9 (8.9 ± 0.25 -fold), Caspase 3 (7.6 ± 0.03 -fold), Bax (1.5 ± 0.09 -fold), p53 (1.89 ± 0.21 -fold), p21 (1.7 ± 0.23 -fold), and Puma (1.22 ± 0.03 -fold), was observed at 10^{-6} M concentration after 6 h, whereas antiapoptotic genes such as Bcl₂ (0.7 ± 0.06 -fold), Bclw (0.8 ± 0.06 -fold), and Mcl1 (0.8 ± 0.05 -fold) were significantly downregulated. Out of the 14 genes studied, the level of expression of four genes, viz., BclxL, Bid, Bnip3, and Bak were not altered significantly following MCP exposure (Figure 7).

Translational Changes. Genes showing significant alterations at the transcriptional level were studied further to determine the alterations in the expression at protein level (Figure 8). In general, MCP (10^{-6} M) exposure for 6 h was found to be most effective in the upregulation of apoptosis marker proteins, viz., Bax (2.66 ± 0.36 -fold), p53 (1.95 ± 0.27 -fold), C-jun (2.04 ± 0.35 -fold), Caspase-9 (1.60 ± 0.21 -fold), and Caspase-3 (1.20 ± 0.094 -fold). Expression of C-fos protein

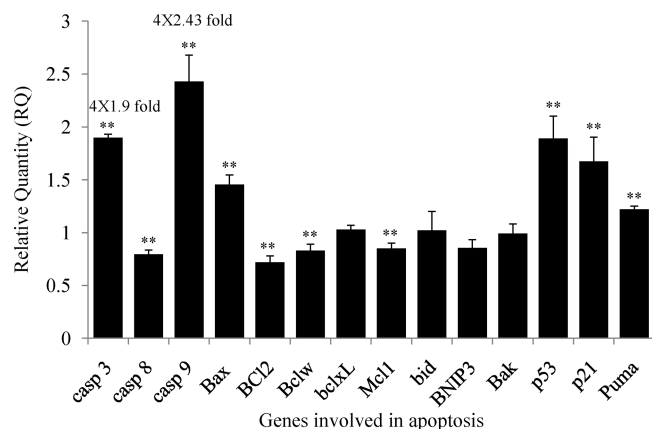


Figure 7. MCP (10^{-6} M) induced alterations in the mRNA expression of marker genes associated with apoptosis in PC12 cells. Quantitative real time PCR (RT-PCR^q) was performed in triplicate by SYBR Green dye using ABI PRISM 7900HT Sequence Detection System (Applied Biosystems, USA). β -Actin was used as the internal control to normalize the data, and MCP induced alterations in mRNA expression are expressed in relative quantity compared with those for the respective unexposed control groups.

was induced in a time-dependent manner, i.e., 2.87 ± 0.34 -, 4.10 ± 0.64 -, and 4.69 ± 0.75 -fold at 6, 12, and 24 h of MCP exposure, respectively. By 12 h of exposure, the expressions were brought down except in the case of Bcl₂ (0.911 ± 0.13 -fold). However, the values were still higher than those of the unexposed basal control. At 24 h, MCP-induced changes in protein expression remained significantly higher than those of the control for Bax, C-fos, C-jun, and p53. However, the expressions of Caspase-9, Caspase-3, and Bcl₂ were down regulated below the basal controls.

In the autorecovery experiment, up to a maximum 100% and a minimum of 19% recovery was observed for Caspase-9 and C-fos, respectively. For Bcl₂, the recovery group showed the expression below the basal control (Figure 8). Autorecovery was found to be statistically significant ($p < 0.001$) for all of the marker proteins studied.

Translocation of Bax and Cytochrome-c. The involvement of mitochondria-mediated pathways in MCP-induced apoptosis was confirmed by the translocation of Bax protein from cytosol to mitochondria, and cytochrome-c protein from mitochondria to cytoplasm using the Western blot technique. MCP (10^{-4} M– 10^{-7} M) exposure for 6 h induced dose-dependent translocation of Bax protein from the cytoplasm to mitochondria, and cytochrome-c from the mitochondria to the cytoplasm (Figure 9). The purity of both the fractions, viz., cytosolic and mitochondrial, was found to be very high. Cross-contamination of the cytosol and mitochondria-specific proteins was not detectable.

Activity of Caspase-9 and Caspase-3. Highlights of MCP-induced alterations in the activity of Caspase-9 and Caspase-3 are shown in Figure 10a and b, respectively. The activity of Caspase-9 was found to be increased with increasing concentrations of MCP at all of the exposure periods, i.e., 6 h, 12 h, and 24 h. Interestingly, maximum induction in the activity of Caspase-9 was recorded at 12 h of exposure, i.e., $115.0 \pm 6.4\%$, $139.0 \pm 7.4\%$, and $156.0 \pm 4.9\%$ following 10^{-7} M, 10^{-6} M, and 10^{-5} M concentrations of MCP, respectively (Figure 10a). Caspase-3 activity was also found to be induced under the influence of MCP exposure in a concentration-dependent manner. However, maximum increase in activity of Caspase-3 was recorded at 6 h of exposure of MCP followed by 12 and 24 h, respectively (Figure 10b). The increase in the activity of both Caspase-9 and Caspase-3 was statistically significant ($p < 0.001$) at 12 h and 6 h, respectively.

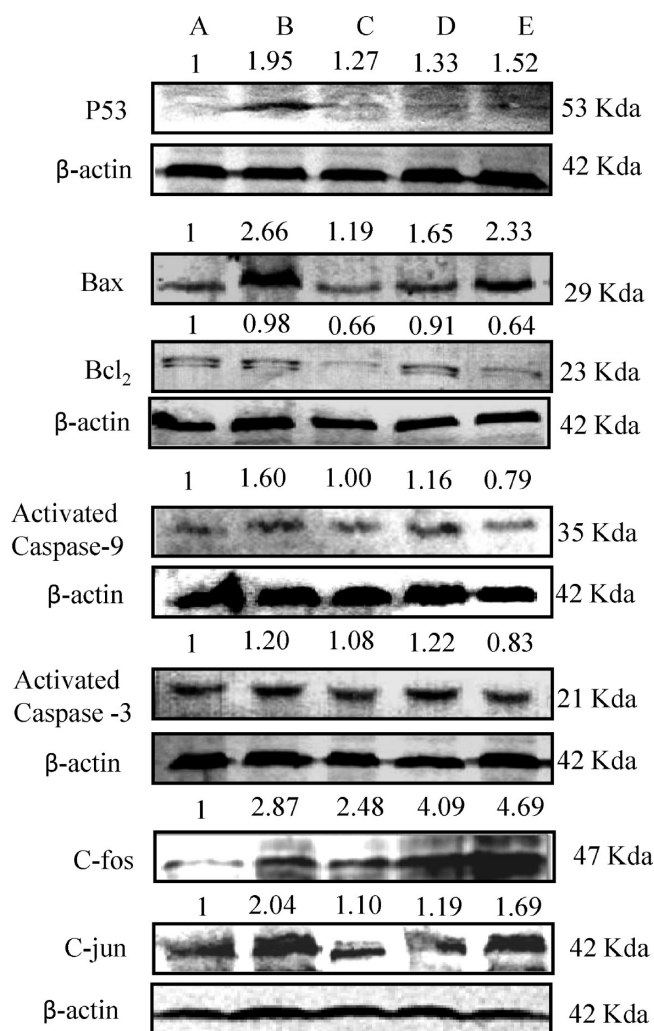


Figure 8. Alterations in the expression of proteins involved in the induction of apoptosis were studied in PC12 cells exposed to MCP (10^{-6} M) for various time periods. β -Actin was used as the internal control to normalize the data. Lane A, untreated control; B, cells exposed to MCP for 6 h; C, proteins isolated after 24 h, i.e., 6 h of MCP exposure + 18 h without exposure (autorecovery period); D, cells exposed to MCP for 12 h; and E, cells exposed to MCP for 24 h. Molecular weight of protein studied: p53 (53 kDa), Bax (29 kDa), Bcl₂ (23 kDa), activated Caspase-9 (35 kDa), activated Caspase-3 (21 kDa), C-fos (47 kDa), C-jun (42 kDa), and β -Actin (42 kDa) for normalization. Relative quantification of alterations in the expression of proteins involved in the induction of apoptosis in PC12 cells exposed to MCP (10^{-6} M) for various time periods. β -Actin was used as the internal control to normalize the data. Quantification was done in Gel Documentation System (Alpha Innotech, USA) with the help of AlphaEase FC StandAlone V.4.0 software.

Discussion

PC12 cells showed evidence of apoptosis by all the four assays employed to assess the cytotoxicity of MCP. Our results indicate that MCP-induced metabolic activation may be primarily due to altered mitochondrial activity since the MTT assay is related to mitochondrial activity and was found to be the most sensitive among the tests employed in this study. Such differences in sensitivity due to organelle specificity of chemicals have already been reported for different toxicants, even in the same cell system (40). In general, the MTT assay is used in studies conducted with organophosphates for cytotoxicity assessment in primary cultures of mouse brain cerebellar cells (16), cultured human peripheral blood lymphocytes (41), daphnia, fish, and rodents (42, 43).

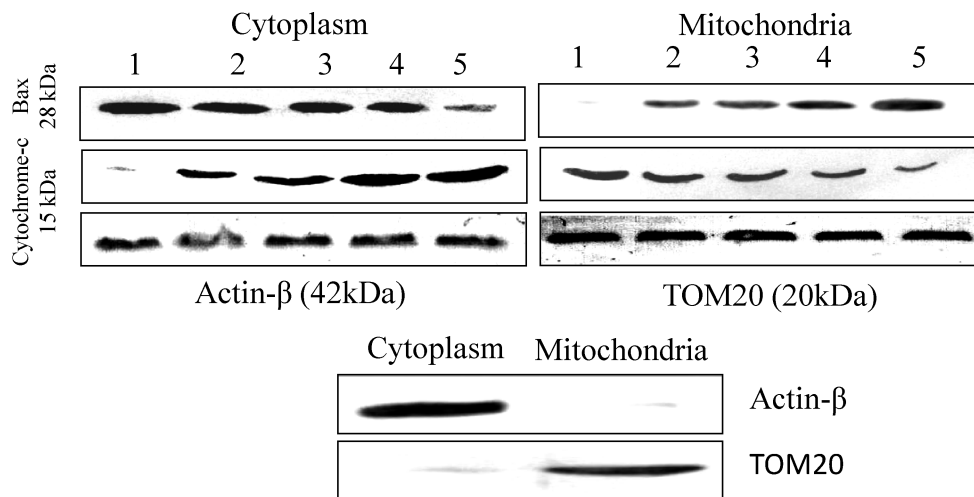


Figure 9. Translocation of cytoplasmic Bax protein to mitochondria and mitochondrial cytochrome-c protein to cytoplasm in PC12 cells following the exposure of various concentrations of MCP for 6 h. Lane 1, untreated control; lane 2, cells exposed to 10^{-7} M of MCP; lane 3, cells exposed to 10^{-6} M of MCP; lane 4, cells exposed to 10^{-5} M of MCP; lane 5, cells exposed to 10^{-4} M of MCP. TOM20 and β -Actin were used to assess the purity of proteins isolated from mitochondria and cytoplasm, respectively.

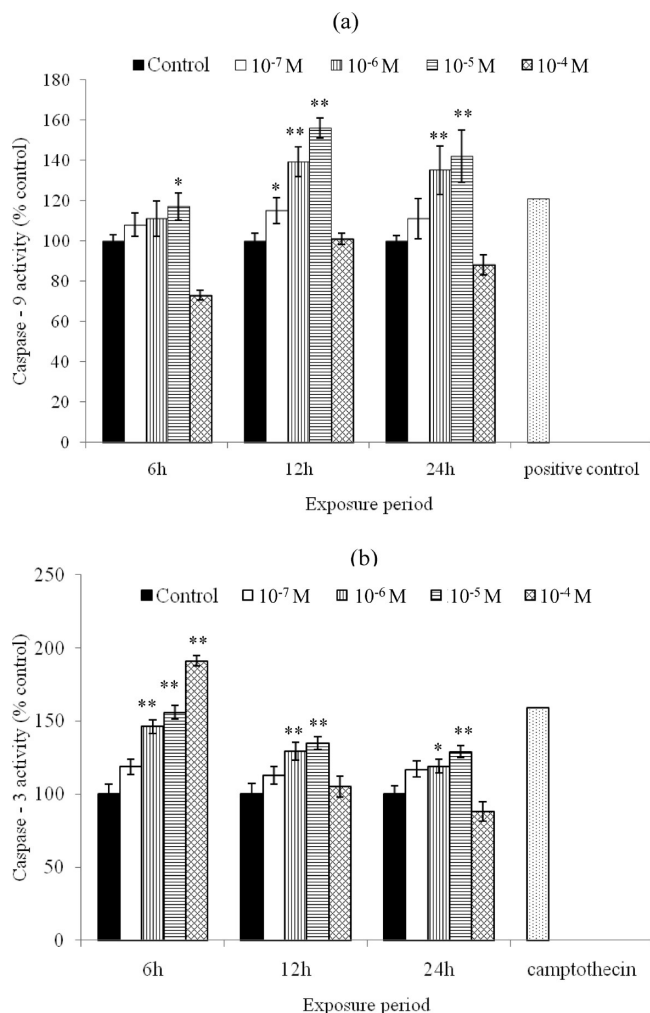


Figure 10. (a) Induction in the activity of Caspase-9 in PC-12 cells exposed to MCP (10^{-4} – 10^{-7} M) for different time periods. Positive control was recombinant Caspase-9 (provided with the kit by manufacturer). * = $P < 0.05$; ** = $p < 0.001$. (b) Induction in the activity of Caspase-3 in PC-12 cells exposed to MCP 10^{-4} – 10^{-7} M) for different time periods. (Positive control (cells exposed with Camptothecin (1 μ g/mL)) for 24 h.) * = $P < 0.05$; ** = $p < 0.001$.

Because of high lipid contents, brain cells are highly vulnerable to xenobiotics-induced oxidative stress leading to

high oxygen consumption and low levels of glutathione content (44, 45). ROS generation is considered to be one of the key signals for oxidative stress-induced apoptosis (46). In our study, significant ($p < 0.001$) generation of ROS, LPO, and increased ratio of GSSG/GSH were observed in PC12 exposed to selected doses of MCP. The generation of ROS has been reported to enhance the ratio of GSSG/GSH and LPO production, which eventually leads to apoptosis in a variety of cells such as astrocytes (47) and PC12 cells (48), and in tissues, such as the rat brain (49, 50). Organochlorine pesticides are also reported to induce ROS generation, which subsequently leads to apoptosis and cell death in mice (51), blood mononuclear cells (52), and mouse macrophage cell lines (29). Thus, ROS generation in the present study may be a mediator for MCP-induced apoptosis in PC12 cells. We confirmed the involvement of ROS in MCP-induced apoptosis by using an ROS inhibitor, which reverses apoptosis (data not shown).

DNA laddering, MN, and TUNEL assays suggest that exposure of cells to higher concentrations of MCP for a longer period of time may reduce the apoptotic cell counts due to increased necrotic cell death. The conversion of apoptosis to necrosis has been demonstrated following the exposure of high concentrations of toxicants for lower time periods and lower concentrations for longer time periods (53, 54). Our results support this phenomenon, as apoptosis observed following MCP exposure was characterized by DNA fragments of low molecular weight, possibly due to inter-nucleosomal cleavage of the chromatin into 180- to 200-bp fragments (55). Apoptosis turned into necrosis after 24 h of exposure as indicated by the detection of a gap in high molecular weight DNA fragmentations. FACS analysis with labeled cells also confirms our findings of DNA fragmentation. A similar pattern of DNA fragmentation has also been demonstrated in the case of apoptotic and necrotic cell death following the exposure of chemicals of different groups (56, 57).

The involvement of mitochondrial chain complexes in ROS-induced apoptotic changes in cytoplasm has been reported (58). Such apoptotic changes are known to follow different pathways (46, 59–62). Organophosphates including paraoxon, parathion, PSP, TOTP, and TPPi induced apoptosis is associated with nuclear condensation, budding and fragmentation, Caspase-3 activation, and DNA fragmentations in SHY-SY-5Y, a human neuroblastoma cell line (63). We observed that MCP significantly upregulated in the expression (both mRNA and protein)

of Caspase-3, caspase-9, Bax, p53, P21, Puma, and downregulated Bcl₂, Bclw, and Mcl1. In general, transcriptional changes were well coordinated with translational changes and with physiological activity in the case of Caspase-3 and Caspase-9. Upregulation of nuclear p53 protein is known to play an important role in minimizing DNA damage by inducing transcriptional reprogramming, which finally leads to controlled cell death (64–66). However, high levels of cytoplasmic p53 protein interact with mitochondria, thereby promoting mitochondrial membrane permeabilization (67), and play a key role in the regulation of apoptosis (68). This cytoplasmic p53 protein has been suggested to induce pro-apoptotic members of the Bcl₂ family such as Bax and Bak and their displacement with antiapoptotic Bcl-2 proteins such as Bcl₂, Bcl_{XL}, etc. (62). Thus, the alterations in the expression profile of marker genes in this study indicate that p53 triggers the mitochondrial apoptotic cascade in PC12 cells exposed to MCP.

In the present investigations, a dose-dependent increase in the translocation of Bax protein from cytosol to mitochondria and cytochrome-*c* protein from mitochondria to cytosol was observed in MCP exposed cells. These results confirm the induction of cytoplasmic p53 and its role in triggering the pathway of mitochondrial membrane permeability in PC12 cells (Figure 9). To the best of our knowledge, this is the first report on the MCP-induced translocation of Bax and cytochrome-*c* protein in PC12 cells. However, the translocation of Bax protein from cytosol to mitochondria following the exposure of paraoxon (POX: the bioactive metabolite of parathion) and parathion has been reported in murine EL4 T-lymphocytic leukemia cell lines and is an important event in the induction of mitochondria-mediated apoptosis (69). During pro-apoptotic phases, Bax and Bak proteins get embedded in the mitochondrial membrane because of conformational modifications and are known to create permeable channels which allow larger protein molecules to pass through them (70). This phenomenon has led to mitochondrial leakage from the inner membrane and matrix proteins followed by oxidative phosphorylation uncoupling, ROS over generation, and mitochondrial transmembrane potential dissipation (46). The role of Puma protein has recently been suggested in p53-induced apoptosis (71). The elevated expressions of Puma in the present investigations are therefore in accordance with earlier studies.

Release of cytochrome-*c* (43), HTRA2 (OMI) (72), and DIABLO (SMAC) (73) in the cytoplasm activates Caspase-9 (58), which eventually results in cell death through the cleaving of the executioner caspase, such as Caspase-3. Activated Caspase-3 plays an important role in triggering the catabolic caspase cascade (58). Caspase cascade may be activated through two different pathways, i.e., either by binding of Procaspase-9 with Apaf-1 to form the apoptosome complex following the release of cytochrome-*c* from damaged mitochondria (29) or by activation of caspases through the OMI and SMACs molecules (74). Patterns of expression of apoptosis markers and activity of Caspase-9 and Caspase-3 obtained in the present investigations are indicative of mitochondria-mediated apoptosis, which operates through caspase cascade. This is the first report showing mitochondria-mediated apoptosis in MCP exposed PC12 cells. However, the caspase-mediated apoptotic changes following exposure to acetofenate, an organo-chlorinated pesticide, and 4-hydroxynonenal have already been reported in macrophages (29) and PC12 cells, respectively (75). On the basis of our findings, we propose a hypothetical model on the apoptotic effects of MCP on PC12 cells (Figure 11). In this scheme, MCP first triggers intrinsic generation of ROS, which subsequently initiates oxidative damage. The increased ROS levels and genotoxicity up regulate p53 and attenuate Bcl-2 protein, leading to a declined ratio of Bcl-

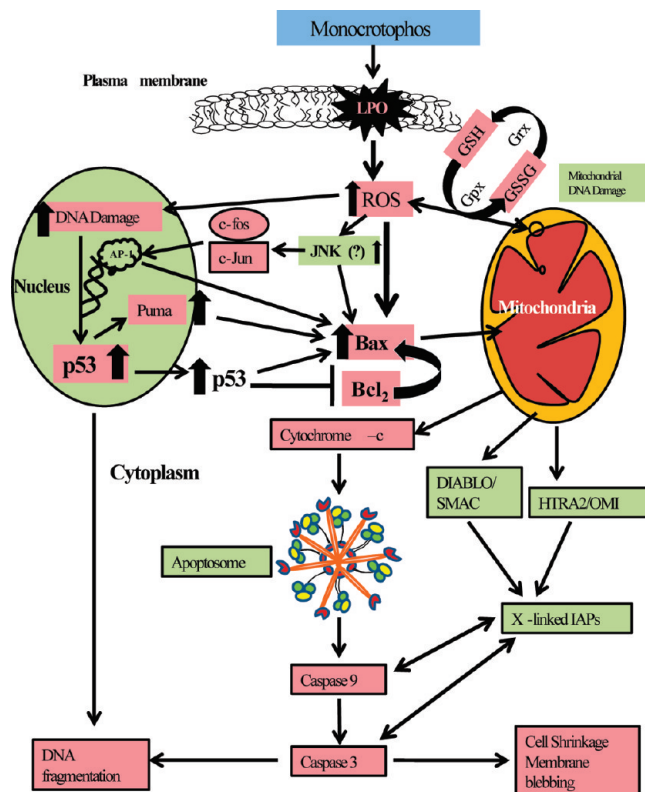


Figure 11. Schematic flow diagram to depict the MCP induced apoptotic pathway in PC12 cells.

2/Bax. The alteration of Bcl₂/Bax ratio results in the release of cytochrome *c*. Finally, the release of cytochrome-*c* activates Caspase-9 and subsequently triggers the Caspase-3 cascade leading to apoptosis in PC12 cells.

Conclusions

To our knowledge, MCP (a widely used organophosphate pesticide) induced the apoptosis in rat neuronal PC12 cells. Apoptotic damages were mitochondria-mediated and regulated through caspase cascade (Caspase-9 and Caspase-3). Our data provides insights into MCP-induced apoptotic cell death in neuronal cells and the possible cellular and molecular mechanisms involved.

Acknowledgment. We are grateful to the Director, Indian Institute of Toxicology Research, Lucknow, India, for his keen interest in the study. Financial support by Council of Scientific & Industrial Research, New Delhi, (SIP-08) is acknowledged. University Grant Commission, New Delhi is acknowledged for providing the fellowship to Mr. M. P. Kashyap. The technical support by Mr. Rajesh Mishra is also acknowledged. This manuscript is IITR communication # 2787.

Supporting Information Available: Data of cytotoxicity studies (Figure-S1–3); list of primers used in the study (Table-S-1). This material is available free of charge via the Internet at <http://pubs.acs.org>.

References

- Steerenberg, P., van Amelsvoort, L., Colosio, C., Corsini, E., Fustinoni, S., Vergieva, T., Zaikov, C., Pennanen, S., Liesivuori, J., and Van Loveren, H. (2008) Toxicological evaluation of the immune function of pesticide workers, a European wide assessment. *Hum. Exp. Toxicol.* 27, 701–707.

- (2) Li, Q., Kobayashi, M., and Kawada, T. (2009) Chlorpyrifos induces apoptosis in human T cells. *Toxicology* 255, 53–57.
- (3) Costa, L. G. (2006) Current issues in organophosphate toxicology. *Clin. Chim. Acta* 366, 1–13.
- (4) Perera, P. M., Jayamanna, S. F., Hettiarachchi, R., Abeyasinghe, C., Karunatilake, H., Dawson, A. H., and Buckley, N. A. (2009) A phase II clinical trial to assess the safety of clonidine in acute organophosphorus pesticide poisoning. *Trials* 10, 73.
- (5) Montgomery, M. P., Kamel, F., Saldana, T. M., Alavanja, M. C., and Sandler, D. P. (2008) Incident diabetes and pesticide exposure among licensed pesticide applicators: Agricultural Health Study, 1993–2003. *Am. J. Epidemiol.* 167, 1235–1246.
- (6) Andreotti, G., Freeman, L. E., Hou, L., Coble, J., Rusiecki, J., Hoppin, J. A., Silverman, D. T., and Alavanja, M. C. (2009) Agricultural pesticide use and pancreatic cancer risk in the Agricultural Health Study Cohort. *Int. J. Cancer* 124, 2495–2500.
- (7) Mills, K. T., Blair, A., Freeman, L. E., Sandler, D. P., and Hoppin, J. A. (2009) Pesticides and myocardial infarction incidence and mortality among male pesticide applicators in the agricultural health study. *Am. J. Epidemiol.* 170, 892–900.
- (8) Dassanayake, T., Gawarammana, I. B., Weerasinghe, V., Dissanayake, P. S., Pragaash, S., Dawson, A., and Senanayake, N. (2009) Auditory event-related potential changes in chronic occupational exposure to organophosphate pesticides. *Clin. Neurophysiol.* 120, 1693–1698.
- (9) Shenouda, J., Green, P., and Sultatos, L. (2009) An Evaluation of the inhibition of human butyrylcholinesterase and acetylcholinesterase by the organophosphate chlorpyrifos oxon. *Toxicol. Appl. Pharmacol.* 241, 135–142.
- (10) Aurbek, N., Thiermann, H., Szinicz, L., Eyer, P., and Worek, F. (2006) Analysis of inhibition, reactivation and aging kinetics of highly toxic organophosphorus compounds with human and pig acetylcholinesterase. *Toxicology* 224, 91–99.
- (11) Sarabia, L., Maurer, I., and Bustos-Obregon, E. (2009) Melatonin prevents damage elicited by the organophosphorous pesticide diazinon on the mouse testis. *Ecotoxicol. Environ. Saf.* 72, 938–942.
- (12) Poovala, V. S., Huang, H., and Salahudeen, A. K. (1999) Role of reactive oxygen metabolites in organophosphate-bidrin-induced renal tubular cytotoxicity. *J. Am. Soc. Nephrol.* 10, 1746–1752.
- (13) Chan, J. Y., Chan, S. H., Dai, K. Y., Cheng, H. L., Chou, J. L., and Chang, A. Y. (2006) Cholinergic-receptor-independent dysfunction of mitochondrial respiratory chain enzymes, reduced mitochondrial transmembrane potential and ATP depletion underlie necrotic cell death induced by the organophosphate poison mevinphos. *Neuropharmacology* 51, 1109–1119.
- (14) Saulsbury, M. D., Heyliger, S. O., Wang, K., and Round, D. (2008) Characterization of chlorpyrifos-induced apoptosis in placental cells. *Toxicology* 244, 98–110.
- (15) Moore, P. D., Yedjou, C. G., and Tchounwou, P. B. (2009) Malathion-induced oxidative stress, cytotoxicity, and genotoxicity in human liver carcinoma (HepG(2)) cells. *Environ. Toxicol.* 25, 221–226.
- (16) Giordano, G., Afsharinejad, Z., Guizzetti, M., Vitalone, A., Kavanagh, T. J., and Costa, L. G. (2007) Organophosphorus insecticides chlorpyrifos and diazinon and oxidative stress in neuronal cells in a genetic model of glutathione deficiency. *Toxicol. Appl. Pharmacol.* 219, 181–189.
- (17) Slotkin, T. A., and Seidler, F. J. (2009) Oxidative and excitatory mechanisms of developmental neurotoxicity: transcriptional profiles for chlorpyrifos, diazinon, dieldrin, and divalent nickel in PC12 cells. *Environ. Health Perspect.* 117, 587–596.
- (18) Roegge, C. S., Timofeeva, O. A., Seidler, F. J., Slotkin, T. A., and Levin, E. D. (2008) Developmental diazinon neurotoxicity in rats: later effects on emotional response. *Brain Res. Bull.* 75, 166–172.
- (19) Veronesi, B., and Ehrlich, M. (1993) Differential cytotoxic sensitivity in mouse and human cell lines exposed to organophosphate insecticides. *Toxicol. Appl. Pharmacol.* 120, 240–246.
- (20) Romero-Navarro, G., Lopez-Aceves, T., Rojas-Ochoa, A., and Fernandez Mejia, C. (2006) Effect of dichlorvos on hepatic and pancreatic glucokinase activity and gene expression, and on insulin mRNA levels. *Life Sci.* 78, 1015–1020.
- (21) Sachana, M., Flaskos, J., Alexaki, E., Glynn, P., and Hargreaves, A. J. (2001) The toxicity of chlorpyrifos towards differentiating mouse N2a neuroblastoma cells. *Toxicol. In Vitro* 15, 369–372.
- (22) Yang, Q. H., Church-Hajduk, R., Ren, J., Newton, M. L., and Du, C. (2003) Omi/HtrA2 catalytic cleavage of inhibitor of apoptosis (IAP) irreversibly inactivates IAPs and facilitates caspase activity in apoptosis. *Genes Dev.* 17, 1487–1496.
- (23) Jin, H. O., Park, I. C., An, S., Lee, H. C., Woo, S. H., Hong, Y. J., Lee, S. J., Park, M. J., Yoo, D. H., Rhee, C. H., and Hong, S. I. (2006) Up-regulation of Bak and Bim via JNK downstream pathway in the response to nitric oxide in human glioblastoma cells. *J. Cell Physiol.* 206, 477–486.
- (24) Kuan, C. Y., Whitmarsh, A. J., Yang, D. D., Liao, G., Schloemer, A. J., Dong, C., Bao, J., Banasiak, K. J., Haddad, G. G., Flavell, R. A., Davis, R. J., and Rakic, P. (2003) A critical role of neural-specific JNK3 for ischemic apoptosis. *Proc. Natl. Acad. Sci. U.S.A.* 100, 15184–15189.
- (25) Endo, H., Kamada, H., Nito, C., Nishi, T., and Chan, P. H. (2006) Mitochondrial translocation of p53 mediates release of cytochrome c and hippocampal CA1 neuronal death after transient global cerebral ischemia in rats. *J. Neurosci.* 26, 7974–7983.
- (26) Singh, S., Ranjit, A., Parthasarathy, S., Sharma, N., and Bambery, P. (2004) Organo-phosphate induced delayed neuropathy: report of two cases. *Neurol. India* 52, 525–526.
- (27) Singh, M., Sandhir, R., and Kiran, R. (2004) In vitro effects of organophosphate pesticides on rat erythrocytes. *Indian J. Exp. Biol.* 42, 292–296.
- (28) Masoud, A., Kiran, R., and Sandhir, R. (2009) Impaired mitochondrial functions in organophosphate induced delayed neuropathy in rats. *Cell Mol. Neurobiol.* 29, 1245–1255.
- (29) Zhao, M., Zhang, Y., Wang, C., Fu, Z., Liu, W., and Gan, J. (2009) Induction of macrophage apoptosis by an organochlorine insecticide acetofenatate. *Chem. Res. Toxicol.* 22, 504–510.
- (30) Lepsch, L. B., Munhoz, C. D., Kawamoto, E. M., Yshii, L. M., Lima, L. S., Curi-Boaventura, M. F., Salgado, T. M., Curi, R., Planeta, C. S., and Scavone, C. (2009) Cocaine induces cell death and activates the transcription nuclear factor kappa-b in pc12 cells. *Mol. Brain* 2, 3.
- (31) Sarid, R., Ben-Moshe, T., Kazimirsky, G., Weisberg, S., Appel, E., Kobiler, D., Lustig, S., and Brodie, C. (2001) vFLIP protects PC-12 cells from apoptosis induced by Sindbis virus: implications for the role of TNF-alpha. *Cell Death Differ.* 8, 1224–1231.
- (32) Li, Y., and Maret, W. (2009) Transient fluctuations of intracellular zinc ions in cell proliferation. *Exp. Cell Res.* 315, 2463–2470.
- (33) Pant, A. B., Agarwal, A. K., Sharma, V. P., and Seth, P. K. (2001) In vitro cytotoxicity evaluation of plastic biomedical devices. *Hum. Exp. Toxicol.* 20, 412–417.
- (34) Siddiqui, M. A., Singh, G., Kashyap, M. P., Khanna, V. K., Yadav, S., Chandra, D., and Pant, A. B. (2008) Influence of cytotoxic doses of 4-hydroxynonenal on selected neurotransmitter receptors in PC-12 cells. *Toxicol. in Vitro* 22, 1681–1688.
- (35) Halliwell, B., and Whiteman, M. (2004) Measuring reactive species and oxidative damage in vivo and in cell culture: how should you do it and what do the results mean? *Br. J. Pharmacol.* 142, 231–255.
- (36) Srivastava, R. K., Lohani, M., Pant, A. B., and Rahman, Q. (2010) Cytogenotoxicity of amphibole asbestos fibers in cultured human lung epithelial cell line: Role of surface iron. *Toxicol. Ind. Health.* [Online early access], DOI: 10.1177/0748233710374464.
- (37) Schagger, H. (2006) Tricine-SDS-PAGE. *Nat. Protoc.* 1, 16–22.
- (38) Ghosh, S., Patel, N., Rahn, D., McAllister, J., Sadeghi, S., Horwitz, G., Berry, D., Wang, K. X., and Swerdlow, R. H. (2007) The thiazolidinedione pioglitazone alters mitochondrial function in human neuron-like cells. *Mol. Pharmacol.* 71, 1695–1702.
- (39) Waterhouse, N. J., Steel, R., Kluck, R., and Trapani, J. A. (2004) Assaying cytochrome C translocation during apoptosis. *Methods Mol. Biol.* 284, 307–313.
- (40) Fotakis, G., and Timbrell, J. A. (2006) In vitro cytotoxicity assays: comparison of LDH, neutral red, MTT and protein assay in hepatoma cell lines following exposure to cadmium chloride. *Toxicol. Lett.* 160, 171–177.
- (41) Das, P. P., Shaik, A. P., and Jamil, K. (2007) Genotoxicity induced by pesticide mixtures: in-vitro studies on human peripheral blood lymphocytes. *Toxicol. Ind. Health* 23, 449–458.
- (42) Benjamin, N., Kushwah, A., Sharma, R. K., and Katiyar, A. K. (2006) Histopathological changes in liver, kidney and muscles of pesticides exposed malnourished and diabetic rats. *Indian J. Exp. Biol.* 44, 228–232.
- (43) Wang, S., Yan-Neale, Y., Cai, R., Alimov, I., and Cohen, D. (2006) Activation of mitochondrial pathway is crucial for tumor selective induction of apoptosis by LAQ824. *Cell Cycle* 5, 1662–1668.
- (44) Aschner, M., Allen, J. W., Kimelberg, H. K., LoPachin, R. M., and Streit, W. J. (1999) Glial cells in neurotoxicity development. *Annu. Rev. Pharmacol. Toxicol.* 39, 151–173.
- (45) Rossi, D. J., Brady, J. D., and Mohr, C. (2007) Astrocyte metabolism and signaling during brain ischemia. *Nat. Neurosci.* 10, 1377–1386.
- (46) Kroemer, G., Galluzzi, L., and Brenner, C. (2007) Mitochondrial membrane permeabilization in cell death. *Physiol. Rev.* 87, 99–163.
- (47) Zhang, J., Hu, J., Ding, J. H., Yao, H. H., and Hu, G. (2005) 6-Hydroxydopamine-induced glutathione alteration occurs via glutathione enzyme system in primary cultured astrocytes. *Acta Pharmacol. Sin.* 26, 799–805.
- (48) Slotkin, T. A., MacKillop, E. A., Ryde, I. T., Tate, C. A., and Seidler, F. J. (2007) Screening for developmental neurotoxicity using PC12 cells: comparisons of organophosphates with a carbamate, an organochlorine, and divalent nickel. *Environ. Health Perspect.* 115, 93–101.
- (49) Slotkin, T. A., and Seidler, F. J. (2007) Comparative developmental neurotoxicity of organophosphates in vivo: transcriptional responses

- of pathways for brain cell development, cell signaling, cytotoxicity and neurotransmitter systems. *Brain Res. Bull.* 72, 232–274.
- (50) Gonzalez-Santiago, L., Suarez, Y., Zarich, N., Munoz-Alonso, M. J., Cuadrado, A., Martinez, T., Goya, L., Iradi, A., Saez-Tormo, G., Maier, J. V., Moorthy, A., Cato, A. C., Rojas, J. M., and Munoz, A. (2006) Aplidin induces JNK-dependent apoptosis in human breast cancer cells via alteration of glutathione homeostasis, Rac1 GTPase activation, and MKP-1 phosphatase downregulation. *Cell Death Differ.* 13, 1968–1981.
- (51) Sun, F., Anantharam, V., Latchoumycandane, C., Kanthasamy, A., and Kanthasamy, A. G. (2005) Diethylstilbestrol induces ubiquitin-proteasome dysfunction in alpha-synuclein overexpressing dopaminergic neuronal cells and enhances susceptibility to apoptotic cell death. *J. Pharmacol. Exp. Ther.* 315, 69–79.
- (52) Perez-Maldonado, I. N., Herrera, C., Batres, L. E., Gonzalez-Amaro, R., Diaz-Barriga, F., and Yanez, L. (2005) DDT-induced oxidative damage in human blood mononuclear cells. *Environ. Res.* 98, 177–184.
- (53) Huk, O. L., Catelas, I., Mwale, F., Antoniou, J., Zukor, D. J., and Petit, A. (2004) Induction of apoptosis and necrosis by metal ions in vitro. *J. Arthroplasty* 19, 84–87.
- (54) Saini, K. S., Thompson, C., Winterford, C. M., Walker, N. I., and Cameron, D. P. (1996) Streptozotocin at low doses induces apoptosis and at high doses causes necrosis in a murine pancreatic beta cell line, INS-1. *Biochem. Mol. Biol. Int.* 39, 1229–1236.
- (55) Evans, R., and Cidlowski, J. (1995) Apoptosis: Cellular Signaling and Molecular Mechanisms, in *Cell Biology of Trauma* (Lemasters, J., and Oliver, C., Eds.) pp 25–47, CRC Press, Boca Raton, FL.
- (56) Grasl-Kraupp, B., Ruttikay-Nedecky, B., Koudelka, H., Bukowska, K., Bursch, W., and Schulte-Hermann, R. (1995) In situ detection of fragmented DNA (TUNEL assay) fails to discriminate among apoptosis, necrosis, and autolytic cell death: a cautionary note. *Hepatology* 21, 1465–1468.
- (57) Charriaut-Marlangue, C., and Ben-Ari, Y. (1995) A cautionary note on the use of the TUNEL stain to determine apoptosis. *NeuroReport* 7, 61–64.
- (58) Galluzzi, L., Blomgren, K., and Kroemer, G. (2009) Mitochondrial membrane permeabilization in neuronal injury. *Nat. Rev. Neurosci.* 10, 481–494.
- (59) Segui, B., and Legembre, P. (2010) Redistribution of CD95 into the lipid rafts to treat cancer cells. *Recent Pat. Anti-Cancer Drug Discovery* 5, 22–8.
- (60) Poplawski, T., Pawlowska, E., Wisniewska-Jarosinska, M., Ksiazek, D., Wozniak, K., Szczepanska, J., and Blasiak, J. (2009) Cytotoxicity and genotoxicity of glycidyl methacrylate. *Chem.-Biol. Interact.* 180, 69–78.
- (61) Namazi, M. (2009) Cytochrome-P450 enzymes and autoimmunity: expansion of the relationship and introduction of free radicals as the link. *J. Autoimmune Dis.* 6, 4.
- (62) Galluzzi, L., Morselli, E., Kepp, O., Tajeddine, N., and Kroemer, G. (2008) Targeting p53 to mitochondria for cancer therapy. *Cell Cycle* 7, 1949–1955.
- (63) Carlson, K., Jortner, B. S., and Ehrlich, M. (2000) Organophosphorus compound-induced apoptosis in SH-SY5Y human neuroblastoma cells. *Toxicol. Appl. Pharmacol.* 168, 102–113.
- (64) Bunz, F., Dutriaux, A., Lengauer, C., Waldman, T., Zhou, S., Brown, J. P., Sedivy, J. M., Kinzler, K. W., and Vogelstein, B. (1998) Requirement for p53 and p21 to sustain G2 arrest after DNA damage. *Science* 282, 1497–1501.
- (65) Bargonetti, J., and Manfredi, J. J. (2002) Multiple roles of the tumor suppressor p53. *Curr. Opin. Oncol.* 14, 86–91.
- (66) Cui, Q., Yu, J. H., Wu, J. N., Tashiro, S., Onodera, S., Minami, M., and Ikejima, T. (2007) P53-mediated cell cycle arrest and apoptosis through a caspase-3-independent, but caspase-9-dependent pathway in oridonin-treated MCF-7 human breast cancer cells. *Acta Pharmacol. Sin.* 28, 1057–1066.
- (67) Moll, U. M., Wolff, S., Speidel, D., and Deppert, W. (2005) Transcription-independent pro-apoptotic functions of p53. *Curr. Opin. Cell Biol.* 17, 631–636.
- (68) Yu, J., and Zhang, L. (2005) The transcriptional targets of p53 in apoptosis control. *Biochem. Biophys. Res. Commun.* 331, 851–858.
- (69) Saleh, A. M., Vijayarath, C., Masoud, L., Kumar, L., Shahin, A., and Kambal, A. (2003) Paraoxon induces apoptosis in EL4 cells via activation of mitochondrial pathways. *Toxicol. Appl. Pharmacol.* 190, 47–57.
- (70) Dejean, L. M., Martinez-Caballero, S., Guo, L., Hughes, C., Tejjido, O., Ducret, T., Ichas, F., Korsmeyer, S. J., Antonsson, B., Jonas, E. A., and Kinnally, K. W. (2005) Oligomeric Bax is a component of the putative cytochrome c release channel MAC, mitochondrial apoptosis-induced channel. *Mol. Biol. Cell* 16, 2424–2432.
- (71) Wang, P., Yu, J., and Zhang, L. (2007) The nuclear function of p53 is required for PUMA-mediated apoptosis induced by DNA damage. *Proc. Natl. Acad. Sci. U.S.A.* 104, 4054–4059.
- (72) Suzuki, Y., Takahashi-Niki, K., Akagi, T., Hashikawa, T., and Takahashi, R. (2004) Mitochondrial protease Omi/HtrA2 enhances caspase activation through multiple pathways. *Cell Death Differ.* 11, 208–216.
- (73) Deng, Y., Lin, Y., and Wu, X. (2002) TRAIL-induced apoptosis requires Bax-dependent mitochondrial release of Smac/DIABLO. *Genes Dev.* 16, 33–45.
- (74) Wang, X., Zhu, C., Hagberg, H., Korhonen, L., Sandberg, M., Lindholm, D., and Blomgren, K. (2004) X-linked inhibitor of apoptosis (XIAP) protein protects against caspase activation and tissue loss after neonatal hypoxia-ischemia. *Neurobiol. Dis.* 16, 179–189.
- (75) Raza, H., and John, A. (2006) 4-hydroxynonenal induces mitochondrial oxidative stress, apoptosis and expression of glutathione S-transferase A4-4 and cytochrome P450 2E1 in PC12 cells. *Toxicol. Appl. Pharmacol.* 216, 309–318.

TX100234M